

## Complex patterns in reactive microemulsions: Self-organized nanostructures?

Irving R. Epstein<sup>a)</sup> and Vladimir K. Vanag<sup>b)</sup>

*Department of Chemistry and Volen Center for Complex Systems, Brandeis University MS 015, Waltham, Massachusetts 02454-9110*

(Received 14 June 2005; accepted 12 September 2005; published online 30 December 2005)

In a reverse microemulsion consisting of water, oil (octane), an anionic surfactant [aerosol OT (AOT)], and the reactants of the oscillating Belousov-Zhabotinsky (BZ) reaction, a variety of complex spatiotemporal patterns appear. These include traveling and standing waves, spirals that move either toward or away from their centers, spatiotemporal chaos, Turing patterns, segmented waves, and localized structures, both stationary and oscillatory. The system consists of nanometer-sized droplets of water containing the BZ reactants surrounded by a monolayer of AOT, swimming in a sea of oil, through which nonpolar BZ intermediates can diffuse rapidly. We present experimental and computational results on this fascinating system and comment on possible future directions for research. © 2005 American Institute of Physics. [DOI: 10.1063/1.2102447]

**Pattern formation in chemically reacting (reaction-diffusion) systems has become a major area of research since the first report of traveling circular waves in the ferroin-catalyzed Belousov-Zhabotinsky (BZ) reaction.<sup>1</sup> In addition to their aesthetic and intellectual appeal, reaction-diffusion patterns are of interest because of their possible relevance in morphogenesis in living systems.<sup>2</sup> Typical experiments are conducted in a thin layer of aqueous solution, and the patterns obtained are traveling waves that may consist of concentric circles, spirals, or (possibly curved) line segments. Experiments in gels using the chlorite-iodide-malonic acid (CIMA) reaction yield stationary Turing patterns<sup>3</sup> of stripes or spots.<sup>4</sup> In this article, we describe experiments in which the constituents of the Belousov-Zhabotinsky reaction are dispersed in nanometer-sized droplets of water in a reverse microemulsion containing an oil (octane) and the surfactant sodium bis(2-ethylhexyl)sulfosuccinate [aerosol OT (AOT)]. In this BZ-AOT system, we are able to tune the physical structure of the medium by varying the relative concentrations of water, oil, and surfactant. Changing the reactant concentrations allows us to manipulate the chemical properties as well. By scanning through a range of physical and chemical parameters, we generate a remarkable array of patterns, some of them seen for the first time. We present both experimental results and numerical simulations.**

### I. INTRODUCTION

In a tongue-in-cheek letter to the editor of Chemical and Engineering News, a correspondent wrote, "We have recently prepared a nanomaterial in our laboratory that is less than 1 nm across but is capable of sensing the pH of an aqueous solution. In the presence of a sufficient base, it ab-

sorbs light at 550 nm, thus emitting a visible light signal. We plan to call this nanomaterial 'phenolphthalein' subject to a patent search to see if the name is not already in use."<sup>5</sup> Phenolphthalein is, of course, a common indicator used by chemists for decades, if not centuries. The writer was calling attention to what he perceived as the excessive attention being given to nanophenomena in the media and to the fact that all molecules are nanospecies. What determines if a particular molecularly based phenomenon constitutes nanoscience is whether or not structural elements at the nanoscale play a key role in that phenomenon.

One may also wish to distinguish between structures created by self-assembly and those generated via reaction-diffusion dissipative processes.<sup>6</sup> Self-assembled structures occur near or at equilibrium, have a spatial periodicity with a wavelength of the same order of magnitude as the system components, involve physical forces of the order of a few kilojoules, and occur at a minimum of some thermodynamic function of state such as the free energy. They often arise by a process of phase separation and can survive indefinitely without external energy fluxes. Dissipative or dynamical structures associated with chemical concentrations, in contrast, arise only far from equilibrium, can be temporally as well as spatially periodic, have wavelengths two to five orders of magnitude larger than the size of the system components, involve chemical forces (bonds) often tens of kilojoules in magnitude, depend upon reaction rates and the rate of energy dissipation, and require an external flux of energy to compensate for this dissipation. They originate via a dynamic instability, in which a state, often the homogeneous steady state, is unstable to infinitesimal perturbations and transforms to a differently structured state.

The phenomena discussed in this work involve structural features at both the nanometer and micrometer scales and present aspects of both self-assembled and dissipative structures. They involve an oscillatory chemical reaction that has

<sup>a)</sup>Electronic mail: epstein@brandeis.edu

<sup>b)</sup>Electronic mail: vanag@brandeis.edu

been thoroughly studied in the context of dissipative structures, coupled to a self-assembled, unreactive, microemulsion.

## II. THE SYSTEM

### A. The BZ reaction

The BZ reaction is the most thoroughly studied oscillating chemical reaction and serves as a prototype system for a wide range of phenomena in nonlinear chemical dynamics.<sup>7</sup> It consists of the bromination and oxidation of an organic substrate, most often malonic acid (MA), by bromate in the presence of a redox catalyst such as cerium, ferriin, or ruthenium bipyridyl  $[\text{Ru}(\text{bipy})_3]$  in a concentrated solution of sulfuric acid. In an aqueous solution, one can choose concentrations such that the stirred reaction in a beaker will show nearly periodic temporal oscillations, which persist for an hour or so with a period of about 1 min, in the concentrations of the oxidized and reduced forms of the catalyst (as well as other species). In a thin (1–2 mm depth) layer, an unstirred ferriin-catalyzed BZ solution first appears uniformly red (reduced state of ferriin). A small dot of blue (oxidized state) soon appears. This dot expands to a disk whose center then reverts to red until a new dot appears and then expands. Eventually, the original dot becomes the center of a set of concentric blue circles, and other such “pacemakers” appear elsewhere in the medium, serving as sources of other “target patterns.” When waves from two such patterns collide, they annihilate, leaving behind the original red medium. If a circle is broken, e.g., by drawing a needle through the solution, the newly formed ends begin to curl, forming a pair of counter-rotating spiral waves. The points at which pacemakers arise are apparently random, and the waves travel at a constant velocity that depends upon the initial reactant concentrations.

### B. AOT microemulsions

A water-in-oil microemulsion, or reverse microemulsion, is a thermodynamically stable mixture of water, oil, and surfactant, in which the water and surfactant molecules form spherical, nanometer-sized droplets with a polar water core surrounded by a surfactant monolayer. The most widely studied water-in-oil microemulsions employ the surfactant sodium bis(2-ethylhexyl)sulfosuccinate, known as aerosol OT (AOT).<sup>8</sup> The structure of AOT and of a typical droplet, with the polar sulfo group of AOT directed toward the water core and the two branched hydrocarbon tails facing the oil phase, are shown in Fig. 1.

The ratio  $\omega = [\text{H}_2\text{O}]/[\text{AOT}]$  determines the average radius of the water droplet cores, which is roughly equal to  $R_w = 0.17\omega$  (nm). On increasing the volume fraction  $\phi_d$  of the dispersed phase (water plus surfactant), the average distance between the droplets falls and eventually clusters of droplets begin to appear,<sup>9,10</sup> leading to percolation at a critical value  $\phi_p$ , where a sharp increase of about three orders of magnitude in the conductivity occurs.<sup>11</sup> Thus, by varying the composition, one can tune the structural properties of the medium. AOT microemulsions have been used for studying a wide variety of chemically reacting systems.<sup>8</sup>

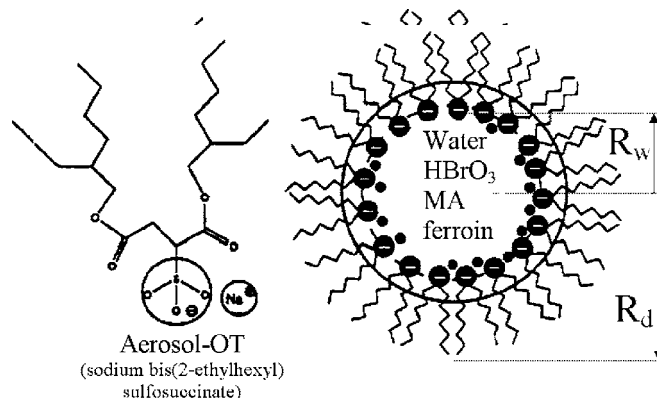


FIG. 1. The AOT molecule (left) and a water droplet containing the BZ reactants surrounded by an oriented monolayer of AOT molecules (right).

### C. The BZ-AOT system

Because the constituents of the BZ system are all quite polar, when they are introduced into an AOT microemulsion, they reside essentially completely within the aqueous droplet phase. Thus, the reaction is confined to the water droplets. The reaction does, however, produce several nonpolar intermediates, the most important of which are Br<sub>2</sub>, which acts as an inhibitor of the reaction, and BrO<sub>2</sub> (or, equivalently Br<sub>2</sub>O<sub>4</sub>), which behaves as an activator. These nonpolar species have a strong tendency to move to the oil and/or surfactant phases. By estimating the partition coefficients of these species between the various phases,<sup>12,13</sup> we can use a set of mass conservation equations to predict their relative amounts in the oil phase. As illustrated in Fig. 2, we find that the amount of inhibitor in the oil phase reaches a maximum at a low droplet fraction, while at high  $\phi_d$  the activator species dominates.

Since the droplets are so small, the diffusion within the droplets is essentially negligible. The polar species then diffuse with entire droplets, with droplets colliding and thereby exchanging materials via fission and fusion. Nonpolar molecules diffuse via ordinary molecular diffusion through the oil phase. Because of these different mechanisms of diffusion, the nonpolar intermediates have diffusion coefficients

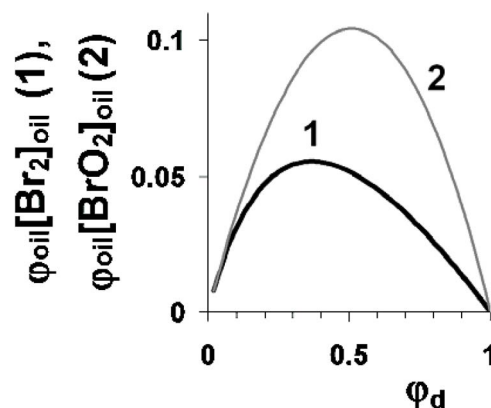


FIG. 2. Calculated amounts of inhibitor (Br<sub>2</sub>) and activator (BrO<sub>2</sub>) in the oil phase of a BZ-AOT system relative to their initial amounts in the water phase.

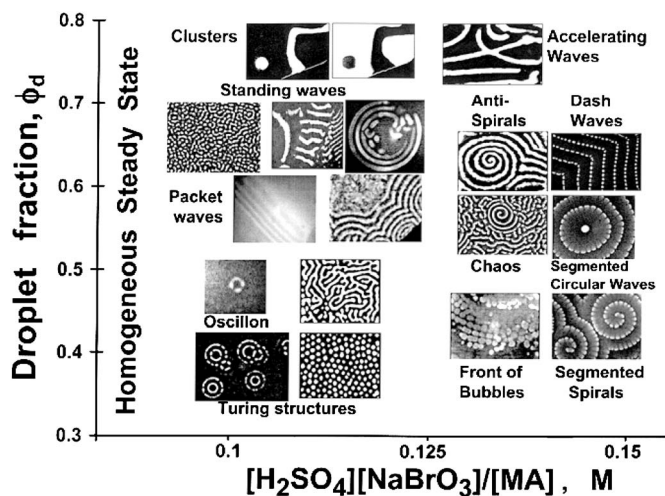


FIG. 3. Schematic overview of patterns found in the BZ-AOT system.

of roughly  $10^{-5}$   $\text{cm}^2/\text{s}$ , while the polar reactants diffuse at rates one to two orders of magnitude slower, since the droplets are much larger than single molecules. Reaction-diffusion systems with such different diffusion coefficients possess unusual properties.<sup>14–16</sup>

We initiate the experiments at 23 °C by mixing equal volumes of two stock microemulsions (MEs) containing the same size and concentration of water droplets. Each ME starts with a 1.5M solution of AOT in octane. ME I is prepared by adding an aqueous solution of  $\text{H}_2\text{SO}_4$  and malonic acid, while ME II is augmented with aqueous ferroin [or another catalyst such as  $\text{Ru}(\text{bipy})_3$  or bathoferroin] and bromate. Microemulsions with different droplet concentrations and the same droplet size can be prepared by dilution with octane.

A small volume of this reactive BZ-AOT mixture is sandwiched between two flat optical windows 50 mm in diameter immediately after mixing the stock MEs. The windows are separated by a 0.1 mm annular Teflon gasket with inner and outer diameters of 20 and 47 mm, respectively, which provides the lateral boundary of the microemulsion and prevents the oil from evaporating. Patterns persist for about 1 h and are observed through a microscope equipped with a digital charge-coupled device (CCD) camera connected to a personal computer. The reaction layer is illuminated by a 40 W tungsten source passing through 450, 510, or 532 nm interference filters for  $\text{Ru}(\text{bipy})_3$ , ferroin, and bathoferroin-catalyzed systems, respectively.

### III. EXPERIMENTAL RESULTS

In Fig. 3, we present an overview of some of the patterns we have observed in the BZ-AOT system. We comment below in more detail on key features of several of these patterns.

#### A. Turing patterns

The stationary reaction-diffusion patterns predicted by Turing<sup>3</sup> in 1952 have inspired a great deal of work in mathematical biology and have provided the initial impetus for our work on the BZ-AOT system. Although the BZ reaction had served as a testing ground for nearly every phenomenon in nonlinear dynamics, it seemed incapable of generating Turing patterns because the reaction involves only small molecules, whose diffusion coefficients do not satisfy the relationship  $D_{\text{inhibitor}}/D_{\text{activator}} \gg 1$  required for Turing patterns. This problem is presumably solved by living organisms by using macromolecules, whose diffusion coefficients can differ quite markedly because of the wide range of molecular masses and sizes. In the CIMA reaction, the starch indicator impregnated in the gel serves as a trap that slows the diffusion of the activator iodine species enough to make the Turing pattern formation possible.<sup>17</sup> In the BZ-AOT system, we have slow-diffusing (water soluble) activator ( $\text{HBrO}_2$ ) and inhibitor ( $\text{Br}^-$ ) and fast-diffusing (oil soluble) activator ( $\text{BrO}_2$ ) and inhibitor ( $\text{Br}_2$ ). Both Turing instability, which produces stationary Turing patterns, and wave instability, which generates wave packets or standing waves,<sup>18</sup> can occur in such a complex system. By carrying out the BZ reaction in an AOT microemulsion at  $\phi_d < \phi_p$  where  $\text{Br}_2$  is the dominant species in the oil phase (Fig. 2), one can create conditions under which Turing instability prevails. The resulting Turing patterns<sup>19</sup> are shown in Fig. 4.

#### B. Spirals and antispirals

Spiral waves are frequently encountered in experiments on aqueous BZ systems. A great deal is known theoretically about the origins of the spiral behavior.<sup>20</sup> Until a set of experiments by Vanag and Epstein<sup>21</sup> in 2001, all reported spirals in reaction-diffusion systems rotated outward from their centers. In these experiments, spirals, dubbed “antispirals,” were found to rotate inward, toward their centers. The emergence of these remarkable antispirals is illustrated in Fig. 5.

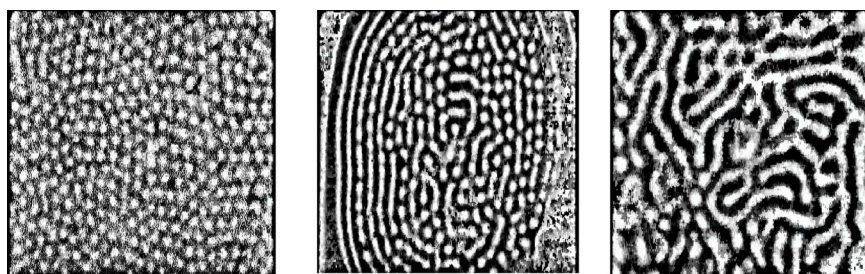


FIG. 4. Turing patterns (from left to right, spots, mixed pattern, stripes) in a BZ-AOT system.



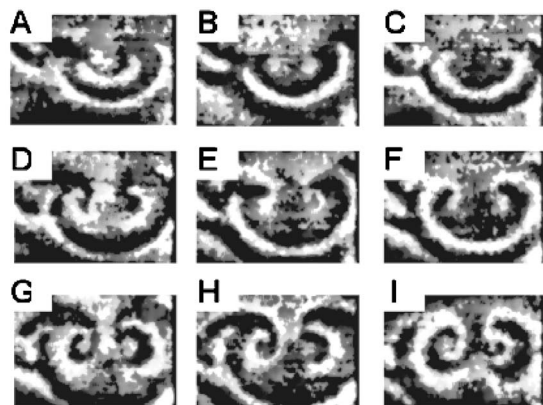


FIG. 5. Emergence of antispirals in the BZ-AOT system. Times (in seconds): (A) 1, (B) 17, (C) 37, (D) 113, (E) 132, (F) 146, (G) 225, (H) 242, and (I) 271. Frame size is  $1.36 \times 0.95$  mm. Each set of three horizontal snapshots shows different stages of antispiral formation during one period (68 s) of bulk oscillations.

### C. Accelerating waves

A related phenomenon, seen under conditions similar to those that support antispirals ( $\phi_d > \phi_p$ ), is referred to as “accelerating waves.”<sup>19</sup> Ordinary BZ waves move at a constant velocity and annihilate upon collision. Accelerating waves instead speed up just before collision and then move apart at right angles subsequent to collision. This behavior, shown in Fig. 6, arises from the additional excitation of the medium in the region between two oncoming waves, a sort of “local explosion” that switches the direction of wave propagation. This behavior resembles somewhat that seen in the collision of traveling spots (particlelike waves).<sup>22</sup>

### D. Segmented waves

In other parameter ranges, plane or nearly plane waves in a BZ-AOT system develop regularly spaced breaks along the wave while continuing to propagate in the transverse direction. The resulting segments grow and then split again when they reach a maximum length. These “dash waves”<sup>23</sup> are seen in Fig. 7.

An even more striking phenomenon, segmented spiral waves,<sup>24</sup> is shown in Fig. 8. In these experiments, ordinary spirals develop in part of the medium, and then dash waves

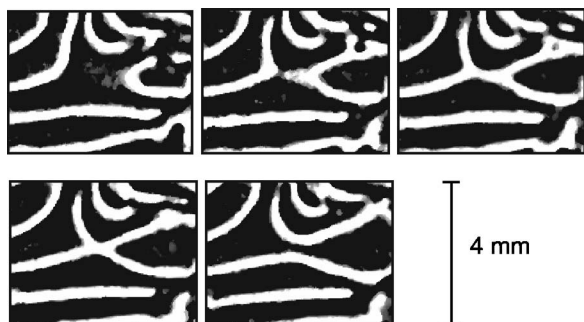


FIG. 6. Accelerating waves in the BZ-AOT system. Times of snapshots, from top left to lower right, are 90, 100, 114, 122, and 134 s.

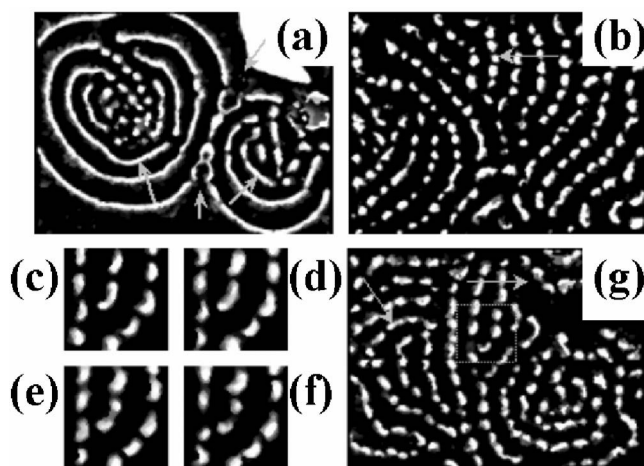


FIG. 7. Dash waves in the BZ-AOT system. Snapshots (b)–(g) are taken, respectively, 1800, 935, 940, 945, 950, and 1000 s after snapshot (a). Dotted square in (g) shows position of snapshots (c)–(f). Large rhomblike white spot in (a) is a fast-propagating phase wave. Arrows show a general direction of wave propagation. Size (mm  $\times$  mm) for (a), (b), (g)  $2.54 \times 1.88$  and for (c)–(f)  $0.53 \times 0.53$ . Wavelength is about 0.19 mm; wave velocity is  $1.5\text{--}2 \mu\text{m/s}$ .

move toward them from another region. The spirals begin to segment, eventually forming structures like that seen in the figure.

### E. Packet waves

Under yet another set of conditions, the BZ-AOT system can support the propagation of finite packets of waves<sup>25</sup> like those shown in Fig. 9. The packets may consist of either plane or circular waves.

### F. Localized structures

With the exception of packet waves, the patterns discussed so far tend to grow to fill the entire medium. One may ask whether the BZ-AOT system might support localized structures, patterns that occupy only a portion of the medium, while the remainder of the system is in a quiescent state. Unlike packet waves which travel, these patterns would remain in a fixed region of space. Such patterns might be either stationary (localized Turing patterns) or oscillatory (“oscillons”). Oscillons have been seen in a variety of physical systems, notably in granular materials,<sup>26</sup> but have not previously been reported in reaction-diffusion systems. With

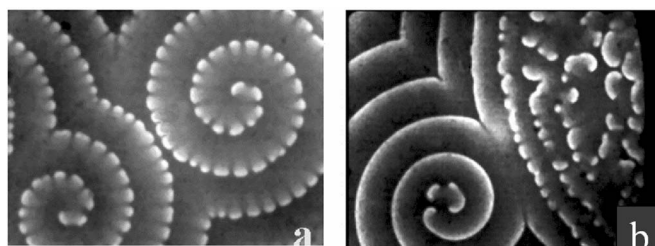


FIG. 8. Segmented spiral waves. (a) Fully developed pair of spirals. (b) Dash waves approach as spiral begins to form segments. Size (mm  $\times$  mm): (a)  $4.82 \times 3.72$ , (b)  $5.0 \times 3.8$ .

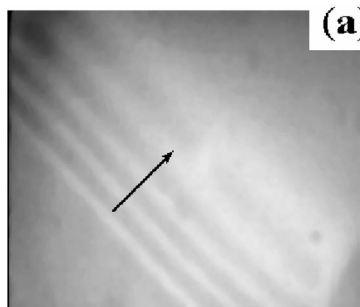


FIG. 9. Packet of plane waves in a BZ-AOT system. Arrow indicates direction of propagation. Size (mm  $\times$  mm): 2.5  $\times$  2.2.

both ferriin and Ru(bipy)<sub>3</sub> catalysts, we find that the BZ-AOT system does indeed exhibit localized structures,<sup>27</sup> some of which are shown in Fig. 10.

#### IV. SIMULATIONS

Essentially all of the experimental behavior described above has been successfully simulated with a set of relatively simple models that capture the key elements of the BZ-AOT system. These features are

- (1) The BZ chemistry. We typically employ a two- or three-variable Oregonator-type model to describe the reactions occurring in the aqueous phase. The key variables represent the concentrations of the activator (HBrO<sub>2</sub>), inhibitor (Br<sup>-</sup>), and catalyst (ferriin).
- (2) Nonpolar intermediates. First-order, reversible reactions are introduced to describe the processes by which activator (BrO<sub>2</sub>) and/or inhibitor (Br<sub>2</sub>) species enter and leave the oil phase, with the ratio of forward and reverse rate constants determined by the partition coefficients of the relevant species. These species undergo an interfacial transfer but do not participate in any chemical reactions.
- (3) Diffusion. To account for the more rapid diffusion of the nonpolar intermediates through the oil phase, the diffusion coefficients for these species are set to values 10–100 times higher than those of the water-based species.

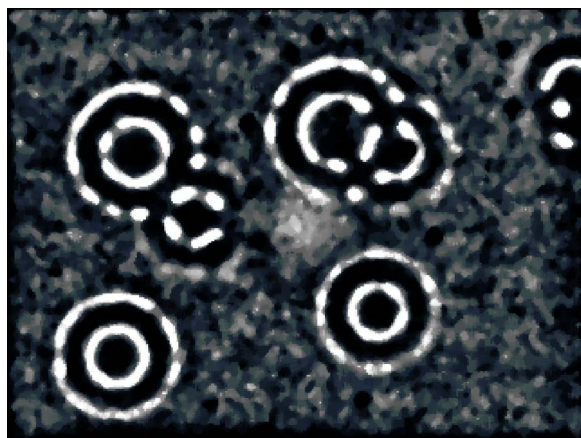


FIG. 10. Localized Turing patterns in a Ru(bipy)<sub>3</sub>-catalyzed BZ-AOT system. Size (mm  $\times$  mm): 5.1  $\times$  3.75.

TABLE I. A model of the BZ-AOT system.

Reactions	Comments
$Y \rightarrow X$	$X = \text{HBrO}_2$ (aq)
$Y + X \rightarrow 0$	$Y = \text{Br}^-$ (aq), $0 =$ inert products
$X \rightarrow 2X + 2Z$	$Z =$ ferriin (aq)
$2X \rightarrow 0$	
$Z \rightarrow hY$	$h =$ stoichiometric coefficient (0.5–2)
$X \rightarrow S$	$S = \text{Br}_2\text{O}_4$ (or $\text{BrO}_2^*$ ) in the oil phase
$S \rightarrow X$	$\text{HBrO}_2 + \text{HBrO}_3 \rightarrow 2\text{BrO}_2^* + \text{H}_2\text{O}$
$Z \rightarrow W$	$W = \text{Br}_2$ in surfactant
$W \rightarrow Z$	
$W \rightarrow U$	$U = \text{Br}_2$ in the oil phase
$U \rightarrow W$	

A detailed model containing six variables is shown in Table I. The first five reactions represent the Oregonator model for the BZ reaction, while the remaining six are interfacial transfer steps. Most of our simulations of specific phenomena employ simplified four-variable models in which (a) the BZ chemistry is reduced to two variables, (b) species residing in the surfactant are neglected, and we include only the activator and the inhibitor in the oil phase.

For details of the individual simulations, we refer the reader to the original papers. We note that linear stability analysis proves to be a useful tool for understanding much of the bifurcation behavior and that the once puzzling phenomenon of inwardly moving waves (e.g., antispirals) is found to be associated with a quantity easily calculated within that framework. When the group velocity or dispersion  $d\omega/dk$ , the derivative of the imaginary part of the eigenvalue of the Jacobian matrix with the most positive real part with respect to the wave number, is negative at the  $k$  for which the real part of that eigenvalue attains its maximum, circular or spiral phase waves move toward their centers while the wave packet as a whole moves away from the point of initial perturbation.<sup>25</sup> A simulated BZ-AOT packet wave in one dimension is shown in Fig. 11.

Simulations have been particularly helpful in understanding the properties and potential applications of localized structures.<sup>27</sup> In Fig. 12 we show that the size of an initial perturbation, which might be generated photochemically in an experimental system, determines whether the perturbation eventually dies out [steady state (SS)], or becomes a stable single localized spot (1T) or oscillon (1O). With multiple perturbations, a much richer behavior, illustrated in Fig. 13, is obtained. Depending on both the width of a pair of initial perturbations and the distance between them, we observe a variety of outcomes including the birth of a third peak, fusion into a single peak, and the annihilation of both peaks. When multiple peaks persist, one or more may be stationary or oscillatory, and oscillatory peaks may be in-phase or out-of-phase. A similar behavior involving fission, fusion, and scattering of localized structures has been reported by Nishiura *et al.*<sup>28</sup>

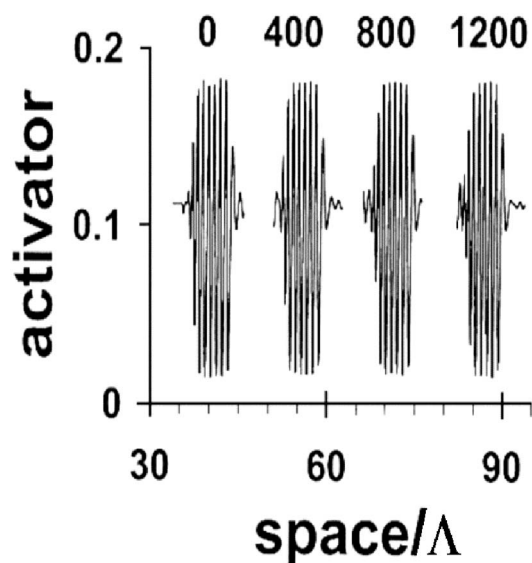


FIG. 11. Propagation of a simulated one-dimensional wave packet. Numbers above wave packets indicate corresponding times. Here  $\Lambda$  is the characteristic wavelength of the wave instability.

## V. CONCLUSIONS

The BZ-AOT system generates a remarkable variety of spatiotemporal patterns. The experiments and simulations reported here are only the first steps in understanding and using the behavior of this fascinating medium. We conclude with several observations about particularly intriguing aspects of this system and about possible future directions for research.

The volume of a single 10 nm diameter droplet is about  $5 \times 10^{-22}$  l. A simple calculation reveals that the average number of molecules per droplet of a species present at 1M concentration is 300. Since the catalyst is typically used at millimolar concentrations, there should be one catalyst molecule *per several droplets!* Clearly, the effects of fluctuations should be enormous in such a medium, and it would be extremely useful to develop a statistical mechanics of systems

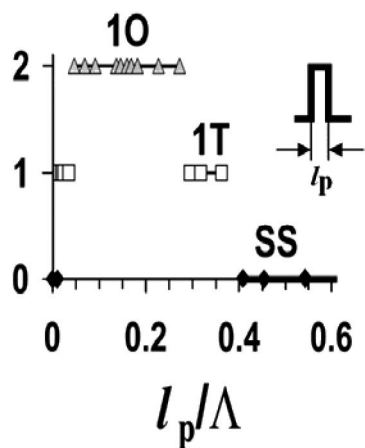


FIG. 12. Simulation of behavior of a localized one-dimensional (1D) perturbation (upper right) as a function of its width  $l_p$ . The ordinate, which distinguishes among states, is arbitrary. Abbreviations: SS, steady state (assigned ordinate value, 0); 1T, single stationary Turing peak (value, 1); 1O, single oscillon (value, 2).

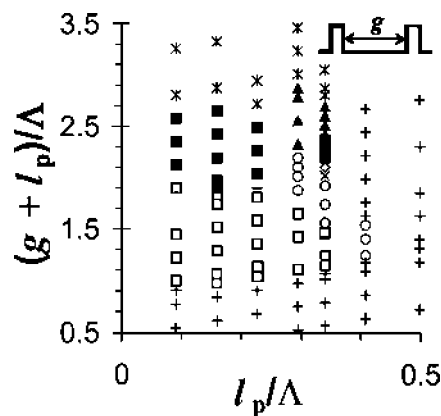


FIG. 13. Simulation of behavior of two identical toothlike initial perturbations separated by a gap of length  $g$  (upper right). Symbols: +, SS; □, oscillon with two synchronously oscillating peaks; ○, stationary Turing pattern with two peaks; ■, oscillon with three synchronously oscillating peaks; ▲, pattern with three peaks, the middle one oscillating and the outer ones stationary ( $T+O+T$ ); ×, single oscillon; −, single stationary peak; ◇, oscillon with two peaks oscillating antiphase; \*, two independent Turing or oscillatory peaks.

consisting of large numbers of subsystems, in each of which large fluctuations are possible. The number of droplets in our simple reactor is of the order of  $10^{15}$ . By varying the diameter of the droplets, we can regulate the magnitude of the intrinsic noise, possibly allowing the emergence of stochastic resonance.<sup>29</sup>

The patterns that we have observed all have wavelengths of one hundred to several hundred micrometers, i.e., four to five orders of magnitude greater than the size of a single droplet. Our observations have been carried out using light microscopy. It is conceivable that structure exists on shorter length scales due to interaction between dissipative and equilibrium self-organized structures, and it may be worth bringing higher-resolution techniques to bear on this question.

The experiments described here all involve the BZ reaction with AOT as the surfactant and octane as the oil. By varying the chemistry, the surfactant, and/or the composition of the oil phase, one may be able to generate new phenomena. We have carried out experiments in which octane is replaced by hexadecane and AOT is supplemented by another surfactant (Span-20). A new wavelength-halving bifurcation has been observed.<sup>30</sup>

It may be worth exploring whether any of the patterns found in the BZ-AOT system can be “frozen in” to generate materials with useful structural properties, e.g., by adding silver salts to produce patterned precipitates of silver bromide.

Coulet *et al.*<sup>31</sup> recently pointed out that media that support localized patterns offer promise for information storage. The simulations presented in Fig. 13 suggest that, by varying how spots are laid down, one may obtain a variety of localized patterns, and the use of photosensitive  $\text{Ru}(\text{bipy})_3$  as the catalyst in the BZ-AOT system makes it feasible to produce any desired initial pattern in the medium.

The periodic (resonant) perturbation of different spatiotemporal patterns in the BZ-AOT system (e.g., by illumi-



nation of the Ru(bipy)<sub>3</sub>-catalyzed system) should yield new patterns and bifurcations.

## ACKNOWLEDGMENTS

This work was supported by grants from the National Science Foundation and the Packard Interdisciplinary Science Program. We thank Lingfa Yang, Akiko Kaminaga, Milos Dolnik, and Anatol Zhabotinsky for their contributions to various aspects of the investigations described here and for many enlightening discussions.

<sup>1</sup>A. N. Zaikin and A. M. Zhabotinsky, *Nature (London)* **225**, 535 (1970).

<sup>2</sup>J. D. Murray, *Mathematical Biology* (Springer-Verlag, Berlin, 1993).

<sup>3</sup>A. M. Turing, *Philos. Trans. R. Soc. London, Ser. B* **237**, 37 (1952).

<sup>4</sup>V. Castets, E. Dulos, J. Boissonade, and P. DeKepper, *Phys. Rev. Lett.* **64**, 2953 (1990).

<sup>5</sup>P. Haberfeld, *Chem. Eng. News* **82**, 6 (2004).

<sup>6</sup>T. Yamaguchi, N. Suematsu, and H. Mahara, *ACS Symp. Ser.* **869**, 16 (2004).

<sup>7</sup>*Oscillations and Traveling Waves in Chemical Systems*, edited by R. J. Field and M. Burger (Wiley, New York, 1985).

<sup>8</sup>T. K. De and A. Maitra, *Adv. Colloid Interface Sci.* **59**, 95 (1995).

<sup>9</sup>M. Almgren and R. Johannsson, *J. Phys. Chem.* **96**, 9512 (1992).

<sup>10</sup>H. Mays, *J. Phys. Chem. B* **101**, 10271 (1997).

<sup>11</sup>M. S. Baptista and C. D. Tran, *J. Phys. Chem. B* **101**, 4209 (1997).

<sup>12</sup>L. Garcia-Rio, J. C. Mejuto, R. Ciri *et al.*, *J. Phys. Chem. B* **103**, 4997 (1999).

<sup>13</sup>Instead of partition coefficients for BrO<sub>2</sub> (which are not available in literature) we use the corresponding partition coefficients for the stable radical ClO<sub>2</sub>, which are approximately 1:1 between the water and oil phases. For Br<sub>2</sub>, the partition coefficients are taken from Ref. 12.

<sup>14</sup>P. K. Becker and R. J. Field, *J. Phys. Chem.* **89**, 118 (1985).

<sup>15</sup>J. A. Sepulchre and V. I. Krinsky, *Chaos* **10**, 826 (2000).

<sup>16</sup>A. von Oertzen, H. H. Rotermund, A. S. Mikhailov, and G. Ertl, *J. Phys. Chem. B* **104**, 3155 (2000).

<sup>17</sup>I. Lengyel and I. R. Epstein, *Science* **251**, 650 (1991).

<sup>18</sup>M. C. Cross and P. C. Hohenberg, *Rev. Mod. Phys.* **65**, 851 (1993).

<sup>19</sup>V. K. Vanag and I. R. Epstein, *Phys. Rev. Lett.* **87**, 228301 (2001).

<sup>20</sup>J. P. Keener and J. J. Tyson, *Physica D* **21**, 307 (1986).

<sup>21</sup>V. K. Vanag and I. R. Epstein, *Science* **294**, 835 (2001).

<sup>22</sup>K. Krischer and A. Mikhailov, *Phys. Rev. Lett.* **73**, 3165 (1994).

<sup>23</sup>V. K. Vanag and I. R. Epstein, *Phys. Rev. Lett.* **90**, 098301 (2003).

<sup>24</sup>V. K. Vanag and I. R. Epstein, *Proc. Natl. Acad. Sci. U.S.A.* **100**, 14635 (2003).

<sup>25</sup>V. K. Vanag and I. R. Epstein, *Phys. Rev. Lett.* **88**, 088303 (2002).

<sup>26</sup>P. B. Umbanhowar, F. Melo, and H. L. Swinney, *Nature (London)* **382**, 793 (1996).

<sup>27</sup>V. K. Vanag and I. R. Epstein, *Phys. Rev. Lett.* **92**, 128301 (2004).

<sup>28</sup>Y. Nishiura, T. Teramoto, and K. I. Ueda, *Chaos* **13**, 962 (2003).

<sup>29</sup>B. Lindner, B. J. Garcia-Ojalvo, A. Neiman, and L. Schimansky-Greier, *Phys. Rep.* **392**, 321 (2004).

<sup>30</sup>A. Kaminaga, V. K. Vanag, and I. R. Epstein, *Phys. Rev. Lett.* **95**, 058302 (2005).

<sup>31</sup>P. Couillet, C. Riera, and C. Tresser, *Chaos* **14**, 193 (2004).